

Fourier transform emission spectroscopy of new infrared systems of LaH and LaD

R. S. Ram

Department of Chemistry, University of Arizona, Tucson, Arizona 85721

P. F. Bernath^{a)}

Department of Chemistry, University of Waterloo, Waterloo, Ontario, Canada N2L 3G1

(Received 20 July 1995; accepted 30 January 1996)

The electronic emission spectra of LaH and LaD have been investigated in the 3 μm –700 nm spectral region using a Fourier transform spectrometer. The molecules were excited in a lanthanum hollow cathode lamp operated with neon gas and a trace of hydrogen or deuterium. The bands observed in the 1 μm –3 μm region have been assigned into two new electronic transitions; $A^1\Pi-X^1\Sigma^+$ and $d^3\Phi-a^3\Delta$. The LaH bands with origins at 4533.5593(8) cm^{-1} and 4430.1916(13) cm^{-1} have been assigned as the 0-0 and 1-1 bands of the $A^1\Pi-X^1\Sigma^+$ transition. The rotational analysis of these bands provides the following principal molecular constants for the ground $X^1\Sigma^+$ state, $B_e=4.080\,534(80)\text{ cm}^{-1}$ and $\alpha_e=0.077\,39(10)\text{ cm}^{-1}$ and $r_e=2.031\,969(20)\text{ \AA}$. To higher wave numbers, three subbands of LaH with origins at 5955.8568(16) cm^{-1} , 6238.3768(8) cm^{-1} , and 6306.6757(15) cm^{-1} have been assigned as the $^3\Phi_2-^3\Delta_1$, $^3\Phi_3-^3\Delta_2$, and $^3\Phi_4-^3\Delta_3$ subbands of the $d^3\Phi-a^3\Delta$ electronic transition. The rotational analysis of the 0-0 and 1-1 bands of the $^3\Phi_2-^3\Delta_1$ and $^3\Phi_4-^3\Delta_3$ subbands and the 0-0, 1-1, and 2-2 bands of the $^3\Phi_3-^3\Delta_2$ subband has been obtained and effective equilibrium constants for the spin components of the $d^3\Phi$ and the $a^3\Delta$ states have been extracted. Magnetic hyperfine structure was also observed in the $a^3\Delta$ state. The rotational analysis of the corresponding LaD transitions has also been carried out and equilibrium constants for the ground and excited states have been determined. The singlet–triplet interval between the $X^1\Sigma^+$ state and the $a^3\Delta$ state is not known but on the basis of *ab initio* calculation and by comparison with LaF and YH, we believe that the ground state of LaH is a $^1\Sigma^+$ state. © 1996 American Institute of Physics. [S0021-9606(96)02517-5]

I. INTRODUCTION

Over the past decade there has been increasing interest in the theoretical and experimental study of transition metal hydrides because of their importance in various areas of science including astrophysics, analytical chemistry, and surface science.^{1–5} Since hydrogen is the most abundant element in the universe, metal hydrides are found in the spectra of sunspots and cool stars. For example, TiH⁶ and FeH^{7,8} have been identified in the spectra of *M*-type stars; NiH⁹ and CrH¹⁰ have been seen in the spectra of sunspots.

There have been numerous theoretical studies of transition metal hydrides in the past decade. These studies focused on the prediction of molecular properties, characterization of low-lying electronic states and understanding the metal hydrogen bond. For all of the 5*d* transition metal hydrides theoretical predictions are available [LaH,¹¹ HfH,¹² TaH,¹³ WH,¹⁴ ReH,¹⁵ OsH,¹⁶ IrH,¹⁷ PtH,¹⁸ and AuH¹⁹]. The experimental data on these molecules are much more limited with electronic spectra of only LaH,^{20,21} HfH,²² WH,²³ PtH,²⁴ and AuH²⁵ molecules available. The visible electronic spectra of LaH have been known since 1975 when Bernard, Bacis, and Zgainski²⁰ observed several bands in the 660–450 nm spectral regions. These bands were classified²¹ into several elec-

tronic transitions which they assigned as $^3\Phi-^3\Delta$, $^1\Delta-^1\Pi$, and $^1\Sigma-^1\Pi$. They were not sure about the nature of the ground electronic state, and based on some erroneous *ab initio* calculations on ScH, they suspected that LaH probably had a $^3\Delta$ ground state. There were no theoretical calculations available at that time for LaH. The electronic spectra of LaH are expected to be very similar to those of YH for which the ground state has been experimentally²⁶ and theoretically established as a $^1\Sigma^+$ state. There is also a well-known similarity between transition metal hydride and fluoride energy levels and LaF has a $^1\Sigma^+$ ground state.²⁷

In recent work²⁶ we have observed the new $e^3\Phi-a^3\Delta$ transition of YH and YD in addition to the previously known $C^1\Sigma^+-X^1\Sigma^+$ transition. Motivated by our YH and YD experiments we decided to search for the corresponding bands of the isovalent LaH and LaD molecules. We observed new bands in the 1–3 μm region which have been classified into two transitions, $A^1\Pi-X^1\Sigma^+$ and $d^3\Phi-a^3\Delta$. The analysis of these transitions will be presented in this paper.

There have been several theoretical calculations of the spectroscopic properties of the IIIB group of transition metal hydrides. A very complete calculation of the properties of the low-lying states of ScH has been published by Anglada *et al.*²⁸ Recently Langhoff *et al.*²⁹ and Balasubramanian and Wang³⁰ have predicted the spectroscopic properties of the low-lying electronic states of YH. These calculations clearly

^{a)}Also: Department of Chemistry, University of Arizona, Tucson, Arizona 85721.

predict ground states of $^1\Sigma^+$ symmetry for ScH and YH. The only theoretical work on the spectroscopic properties of the low-lying electronic states of LaH has been by Das and Balasubramanian.¹¹ They have predicted the energies and spectroscopic properties ($T_e, r_e, \omega_e, \mu_e, D_e$) of many low-lying electronic states of LaH using the complete active space self-consistent field MCSCF(CASSCF) with second-order configuration interaction (SOC) and relativistic configuration interaction (RCI) calculations. This calculation predicts a $^1\Sigma^+$ state as the ground state of LaH with a low-lying $^3\Delta$ first excited state.

Bernard and Bacis²¹ did not observe any transitions having a $^1\Sigma^+$ state as the lower state. Instead they apparently observed two singlet transitions (assigned as $^1\Sigma^-1\Pi$ and $^1\Delta-1\Pi$) having a common lower state. As will be discussed below, their $^1\Pi$ state is in fact the $^3\Delta_1$ spin component of the low-lying $^3\Delta$ state. Das and Balasubramanian¹¹ tried to reassign the transitions observed by Bernard and Bacis²¹ but these new assignments were also not correct. Much of the confusion resulted because all of the transitions observed by Bernard and Bacis²¹ involved excited electronic states. We report here the first measurements on the ground $X^1\Sigma^+$ states of LaH and LaD.

II. EXPERIMENT

The spectra of LaH and LaD molecules were observed in a lanthanum hollow cathode lamp. The cathode was prepared by inserting a 0.13 mm foil of lanthanum metal into a hole in a copper block. The thin, brittle foil made poor contact with the inner cathode walls but LaH and LaD were detected. The lamp was operated at 230 V and 430 mA current and a slow steady flow of 2.3 Torr Ne and about 70 mTorr of H_2 or D_2 was maintained through the lamp.

The spectra were recorded using the 1 m Fourier transform spectrometer associated with the McMath–Pierce Solar Telescope of the National Solar Observatory. The spectra in the 3 500–14 800 cm^{-1} spectral region of LaH were recorded in two experiments. The 3500–9150 cm^{-1} region was recorded using InSb detectors, cold green uranium glass filters and silicon filters with 10 scans coadded in about 70 min of integration. For the 9 100–14 800 cm^{-1} region the spectrometer was operated with a red pass filter (RG715) and Si-diode detectors. A total of 10 scans were coadded in 55 min of integration. In both of these experiments the spectrometer resolution was set at 0.02 cm^{-1} and a CaF_2 beam splitter was used. Since there were no prominent molecular features in the 9 100–14 700 cm^{-1} region in the LaH experiment, we decided to record only the 3 500–9 150 cm^{-1} spectral region of LaD. This time 12 scans were coadded in 80 min of integration. We note that the CaF_2 beam splitter has a poor modulation efficiency above 10 000 cm^{-1} .

The spectral line positions were extracted from the observed spectra using a data reduction program called PC-DECOMP developed by Braut. The peak positions were determined by fitting a Voigt line shape function to each spectral feature.

In addition to the LaH and LaD bands, the spectra also

TABLE I. The correspondence between the labels for the LaH transitions used by Bernard and Bacis (Ref. 21) and the labels adopted in this paper.

Bernard and Bacis	Present work
$^3\Phi_4-^3\Delta_3$	$^3\Phi_4-a^3\Delta_3$
$^3\Phi_3-^3\Delta_2$	$^3\Phi_3-a^3\Delta_2$
$^1\Delta-1\Pi$	$^3\Phi_2-a^3\Delta_1$
$^1\Sigma^+-1\Pi$	$0^+-a^3\Delta_1$

contained La and Ne atomic lines. The La atomic lines have a characteristic hyperfine structure because the ^{139}La atom has a large nuclear spin and a large nuclear magnetic moment ($I=7/2$, $\mu=2.783$ nuclear magnetons). The spectra were calibrated using the measurements of Ne atomic lines made by Palmer and Engleman.³¹ The absolute accuracy of the wavenumber scale is expected to be better than ± 0.001 cm^{-1} . The LaH lines have varying widths because the hyperfine splitting changes with J so that the measurement precision also varies from ± 0.001 to ± 0.003 depending the extent of blending and line broadening.

III. OBSERVATION AND ANALYSIS

The electronic spectrum of LaH is expected to be very similar to that of LaF and to that of the isovalent molecules ScH and YH. The most recent experimental²⁶ and theoretical¹¹ work on YH confirms that the ground state of YH is of $^1\Sigma^+$ symmetry and that the first excited state is of $^3\Delta$ symmetry. For LaH Bernard and Bacis²¹ identified several electronic transitions in the visible region and they assigned two transitions as the $^3\Phi_3-^3\Delta_2$ and $^3\Phi_4-^3\Phi_3$ subbands of a $^3\Phi-^3\Delta$ transition. The third subband, $^3\Phi_2-^3\Delta_1$, was not identified. In addition they identified two additional transitions ($^1\Sigma^-1\Pi$ and $^1\Delta-1\Pi$) with a common $^1\Pi$ state as the lower state. Our work shows that this $^1\Pi$ state is in fact the $^3\Delta_1$ spin component of their lower $^3\Delta$ state which we have denoted as the $a^3\Delta$ state (Table I). This means that none of the transitions observed by Bernard and Bacis²¹ involve the ground $^1\Sigma^+$ state.

In the present work we have observed two new electronic transitions in the infrared; one has a $^1\Sigma^+$ lower state which we have assigned as the $A^1\Pi-X^1\Sigma^+$ transition and the other has a $^3\Delta$ lower state which we have assigned as the $d^3\Phi-a^3\Delta$ transition. The lower state of this transition is the same as the lower state of the $^3\Phi-^3\Delta$ transition of Bernard and Bacis.²¹ A schematic energy level diagram of the electronic states of LaH is provided in Fig. 1. The states marked by the solid lines represent the observed states. The dashed lines represent states that have not been observed yet. The position of these unobserved states and the singlet–triplet splitting (2800 cm^{-1}) are estimated from calculations on LaH¹¹ or LaF.^{27,32} Note that we have no direct experimental evidence that our new $^1\Sigma^+$ state is in fact the ground state of LaH. However, on the basis of the calculation of Das and Balasubramanian¹¹ and by comparison with the YH²⁶ and LaF^{27,32,36} molecules, our assignment is plausible.

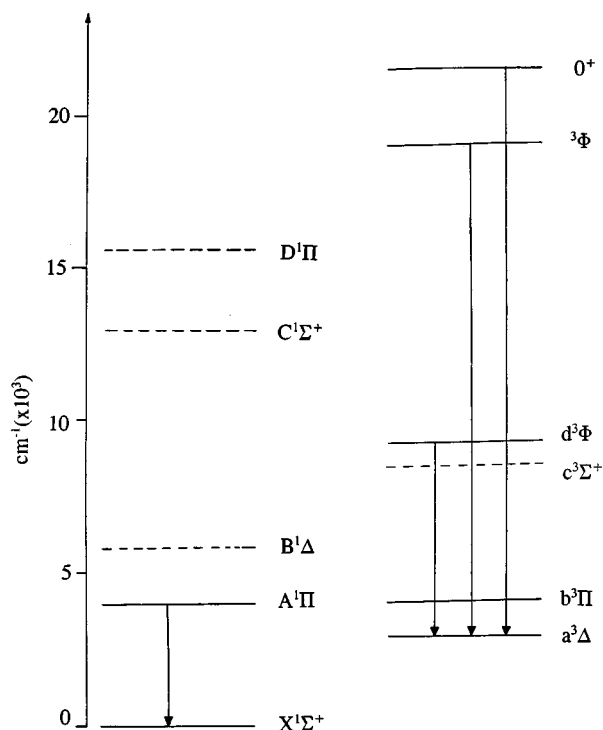


FIG. 1. A schematic energy level diagram of the electronic states of LaH. Dashed lines are predicted energy levels and the singlet-triplet splitting is not reliably known.

The branches in the different bands were picked out using an interactive color Loomis-Wood program running on a PC computer. The different branches were then matched to find the *R* and *P* branches belonging to the same band. Once the *R, P* pair is identified the *J* numbering in these branches was established by adjusting the *J*-assignment until the band origin matched the origin of the *Q*-branch.

A. Spectrum of LaH

The 4000–6500 cm^{-1} region of the LaH spectrum consists of two groups of bands. In the 4000–4600 cm^{-1} region, two bands with origins at 4533.5593(8) cm^{-1} and 4430.1916(13) cm^{-1} have been assigned as the 0-0 and 1-1 bands of the $A^1\Pi-X^1\Sigma^+$ transition. No off-diagonal bands were observed so that the vibrational intervals could not be determined. To higher wave numbers, bands present in the

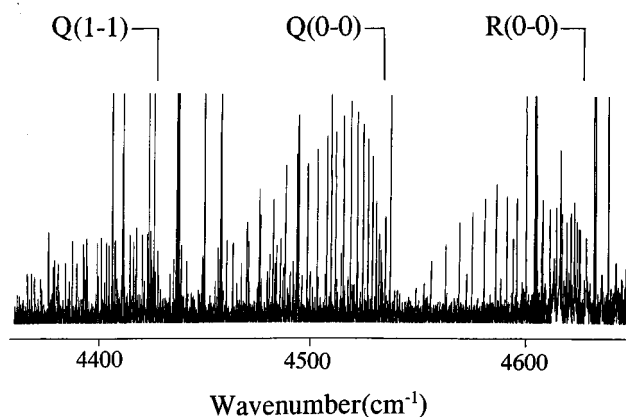


FIG. 2. A portion of the compressed spectrum of the $A^1\Pi-X^1\Sigma^+$ system of LaH.

5600–6500 cm^{-1} region have been classified into three transitions with the 0-0 band origins at 5955.8568(16) cm^{-1} , 6238.3768(8) cm^{-1} , and 6306.6757(15) cm^{-1} . These have been assigned as $^3\Phi_2-^3\Delta_1$, $^3\Phi_3-^3\Delta_2$, and $^3\Phi_4-^3\Delta_3$ subbands of a $^3\Phi-^3\Delta$ transition. The analysis of these two transitions will be described separately.

1. The $A^1\Pi-X^1\Sigma^+$ transition

Each band of this transition consists of a single *R*-, a single *P*-, and a single *Q*-branch with no Ω -doubling as expected for a $^1\Pi-^1\Sigma^+$ transition. The low *J* lines are much broader because of hyperfine structure. For example the widths of the *Q*(1), *Q*(2), *Q*(3), *Q*(4), and *Q*(5) lines are approximately 0.090, 0.080, 0.065, 0.050, and 0.045 cm^{-1} , respectively, in the 0-0 band. The width of the lines is approximately $0.042 \pm 0.001 \text{ cm}^{-1}$ from *Q*(5) to *Q*(12) and then slowly starts increasing again as *J* increases. At *J*=20 the width is approximately 0.075 cm^{-1} and the lines start to appear to have flat tops or even to be split into two components. A compressed part of the spectrum of this transition has been provided in Fig. 2. The *P* branch lines are weaker than the *R*-branch lines and the *Q*-branch is the most intense branch. There is a combination defect observed in the combination differences between *R* and *Q* and *Q* and *P* branches consistent with a $^1\Pi-^1\Sigma^+$ assignment. The lines in the 1-1 band are much weaker than in the 0-0 band. The rotational

TABLE II. Spectroscopic constants (in cm^{-1}) for the $A^1\Pi-X^1\Sigma^+$ system of LaH.

Constants	$X^1\Sigma^+$		$A^1\Pi$	
	$v=0$	$v=1$	$v=0$	$v=1$
T_v	0.0	a	4533.559 33(80)	$a+4430.1916(13)$
B_v	4.041 837(62)	3.964 443(78)	3.876 650(63)	3.798 398(79)
$10^4 \times D_v$	1.338 7(21)	1.333 9(23)	1.281 9(21)	1.248 5(27)
$10^9 \times H_v$	3.12(21)	...	3.55(22)	-1.66(24)
$10^2 \times q_v$	1.145 2(16)	1.119 4(31)
$10^6 \times q_D$	-3.142(83)	-1.93(23)
$10^9 \times q_H$	0.25(11)	-2.32(42)

^aUndetermined.

lines could be followed up to $R(21)$, $P(22)$, and $Q(26)$ in the 0-0 band and up to $R(19)$, $P(14)$, and $Q(21)$ in the 1-1 band. No rotational perturbations were observed these two bands.

The observed line positions were fitted with the following customary energy level expressions for $^1\Sigma^+$ [Eq. (1)] and $^1\Pi$ [Eq. (2)] states,

$$F_v(J) = T_v + B_v J(J+1) - D_v [J(J+1)]^2 + H_v [J(J+1)]^3, \quad (1)$$

$$F_v(J) = T_v + B_v J(J+1) - D_v [J(J+1)]^2 + H_v [J(J+1)]^3 \pm 1/2 \{ q_J [J(J+1) + q_D [J(J+1)]^2 + q_H [J(J+1)]^3 \}. \quad (2)$$

The wave numbers and the assignment of the rotational lines are available from PAPS³³ or from the authors upon request. The constants obtained for the ground and excited states obtained from this fit are provided in Table II.

2. The $d^3\Phi - a^3\Delta$ transition

Each subband of the $d^3\Phi - a^3\Delta$ transition consists of the 0-0 and 1-1 bands. The 2-2 band of the $^3\Phi_3 - ^3\Delta_2$ subband has also been identified and rotationally analyzed. The higher vibrational bands in the other subbands are much weaker in intensity and no off-diagonal bands were observed in our spectra. Each of these bands have P , Q , and R branches and the Ω -doubling is also resolved in the $^3\Phi_2 - ^3\Delta_1$ and $^3\Phi_3 - ^3\Delta_2$ subbands. No satellite branches were observed so that the relative location of the spin components could not be determined.

A part of the $^3\Phi_2 - ^3\Delta_1$ subband showing some low J Q -branch lines is provided in Fig. 3. The Ω -splitting in this subband is fully resolved for lines with $J'' > 4$. In this subband the P -branch lines are weaker in intensity than the R -branch lines and the Q -branch is slightly stronger than the R -branch. The splitting in the rotational lines arises mainly from the larger Ω -doubling in the lower $^3\Delta_1$ state. No rotational perturbations have been observed in the 0-0 and 1-1 bands.

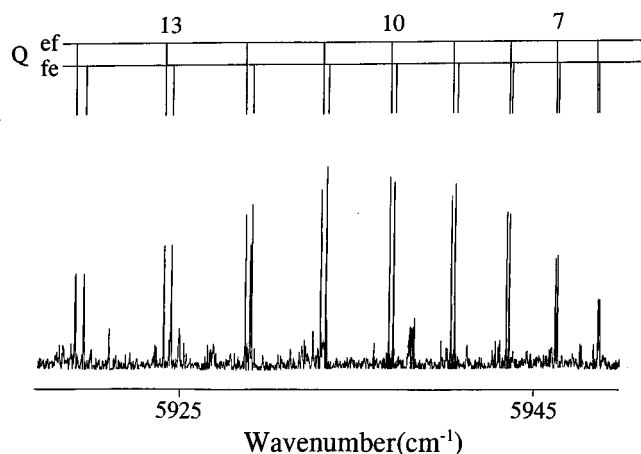


FIG. 3. A portion of the $d^3\Phi_2 - a^3\Delta_1$ subband of LaH near the Q -head.

The subband with an origin at $6238.3768(8)$ cm^{-1} has been identified as $^3\Phi_3 - ^3\Delta_2$. In this subband the intensity of the R -branch is similar to the Q -branch and the P -branch is much weaker. The first lines, $R(2)$, $Q(3)$, and $P(4)$ in the branches can be picked out easily in our spectra confirming the Ω -assignment. The Ω -splitting of the $^3\Phi_3 - ^3\Delta_2$ subband is resolved for lines with $J'' > 14$ and the doubling is much smaller than that in the $^3\Phi_2 - ^3\Delta_1$ subband. Several local perturbations have been observed in the $v=0$ and $v=1$ vibrational levels of the $d^3\Phi_3$ spin component. The perturbation in the $v=0$ vibrational level affects only the f -parity levels at $J'=16$ while the perturbation in the $v=1$ vibrational level affects both the parity levels of the excited state at $J'=9$. Several lines in the vicinity of the perturbation were excluded from the fit.

The next subband to higher wave numbers with an origin at $6306.6757(15)$ cm^{-1} , has been assigned as the $^3\Phi_4 - ^3\Delta_3$ subband. The low JR -, Q -, and P -branch lines are broadened by hyperfine structure and the lines slowly decrease in width with increasing J . In fact the hyperfine structure is nearly completely resolved in the $R(3)$, $R(4)$, and $R(5)$ lines of this

TABLE III. Spectroscopic constants (in cm^{-1}) for the $d^3\Phi - a^3\Delta$ system of LaH.

Constants	$a^3\Delta_1$		$a^3\Delta_2$			$a^3\Delta_3$	
	$v=0$	$v=1$	$v=0$	$v=1$	$v=2$	$v=0$	$v=1$
B_v	3.784 39(14)	3.711 748(88)	3.844 482(29)	3.769 42(19)	3.692 95(17)	3.849 640(58)	3.769 705(68)
$10^4 \times D_v$	1.145 7(74)	1.128 0(22)	1.272 07(71)	1.276 7(75)	1.201 7(55)	1.222 4(11)	1.153 8(11)
$10^9 \times H_v$	3.6(12)	...	3.902(51)	5.73(84)	...	2.421(67)	-2.505(46)
$10^3 \times q_v$	2.080(12)	1.280(21)
$10^6 \times q_{Dv}$	1.173(34)	1.689(79)	-0.072 7(26)
Constants	$d^3\Phi_2$		$d^3\Phi_3$			$d^3\Phi_4$	
	$v=0$	$v=1$	$v=0$	$v=1$	$v=2$	$v=0$	$v=1$
T_{v-v}	5955.8568(16)	5833.4080(28)	6238.3768(8)	6125.4434(21)	6011.8041(33)	6306.6757(15)	6194.0128(33)
B_v	3.614 29(14)	3.542 079(96)	3.635 800(30)	3.560 65(20)	3.482 72(18)	3.692 857(60)	3.612 364(73)
$10^4 \times D_v$	1.329 3(75)	1.327 1(30)	1.252 52(74)	1.269 9(75)	1.150 3(62)	1.364 1(11)	1.317 3(11)
$10^9 \times H_v$	9.7(12)	9.93(37)	2.892(53)	4.96(84)	-9.73(29)	4.325(67)	...
$10^7 \times q_{Dv}$	-1.16(19)	-0.89(27)	-3.922(26)

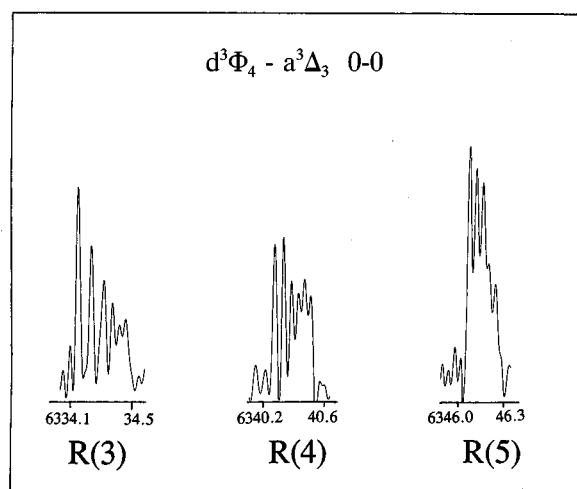


FIG. 4. A portion of the low J R -branch lines of the 0-0 band of $d^3\Phi_4 - a^3\Delta_3$ subband of LaH showing resolved hyperfine structure.

subband (Fig. 4). By comparing R and Q lines with the same J'' value it was found that the hyperfine splitting was present in the lower state $a^3\Delta_3$ spin component, not in the $d^3\Phi_4$ state. The lower state combination differences obtained from the bands of this subband agree well with the corresponding values from the data of Bernard and Bacis²¹ confirming that the same lower state is involved. No rotational perturbations have been observed in any of the analyzed bands.

The hyperfine structure (Fig. 4) shows a typical “flag” pattern characteristic of a_β coupling.³⁴ In this case the hyperfine energy levels³⁴ are given by the expression,

$$\begin{aligned}
 E(J) &= [(a\Lambda + (b+c)\Sigma)]\Omega[F(F+1) - I(I+1) \\
 &\quad - J(J+1)]/[2J(J+1)] \\
 &= [h/2]\Omega[F(F+1) - I(I+1) \\
 &\quad - J(J+1)]/[J(J+1)]
 \end{aligned}
 \tag{3}$$

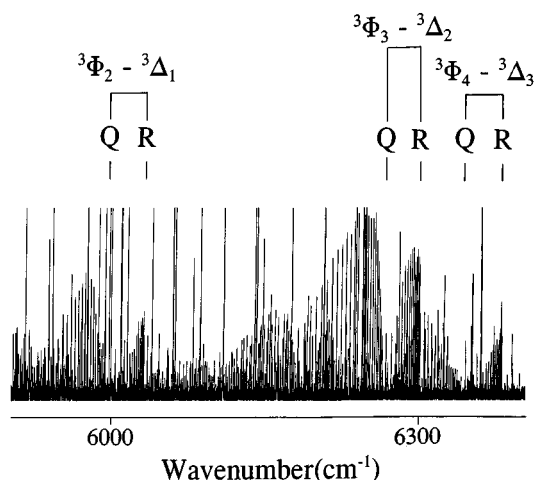


FIG. 5. A portion of the compressed spectrum of the $d^3\Phi - a^3\Delta$ transition of LaD.

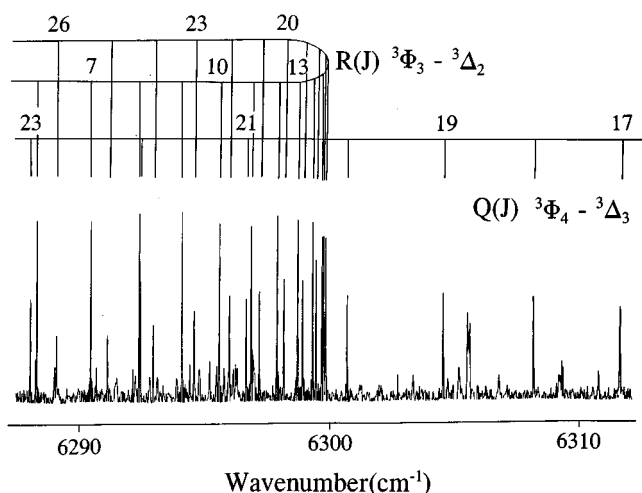


FIG. 6. A portion of the $d^3\Phi_3 - a^3\Delta_2$ 0-0 subband of LaD near the R -head. Some overlapping lines of the $d^3\Phi_4 - a^3\Delta_3$ 0-0 subband have also been marked.

with $h = [a\Lambda + (b+c)\Sigma] = (2a+b+c)$ for a $^3\Delta_3$ spin component. The value of the hyperfine constant h was found to be $+0.053 \text{ cm}^{-1}$. For the lines which show hyperfine splitting, the average line positions were used in the fit with reduced weights.

The observed wave numbers of the different subbands were fitted separately by treating each spin component as a separate Hund's case (c) state. The term energy expression for a Hund's case (c) state is the same as for the $^1\Pi$ state [Eq. (2)].

The observed transition wave numbers of different subbands are available from PAPS³³ or from the authors. The perturbed transitions were excluded from the final fit. The rotational constants obtained from this fit for the $a^3\Delta$ and $d^3\Phi$ states are provided in Table III. The e/f parity assignment has been chosen arbitrarily by putting the e parity level for a given J higher in energy than the f parity level for the $^3\Delta_2$ and $^3\Delta_1$ spin components. The unusual observation of Ω -doubling in the $^3\Delta$ and $^3\Phi$ states is consistent with the Hund's case (c) tendencies of the excited states of LaH. There are both local and global perturbations in the rotational

TABLE IV. Spectroscopic constants (in cm^{-1}) for the $A^1\Pi - X^1\Sigma^+$ system of LaD.

Constants	$X^1\Sigma^+$		$A^1\Pi$	
	$v=0$	$v=1$	$v=0$	$v=1$
T_v	0.0	a	4547.5969(26)	$a+4472.7499(42)$
B_v	2.051 694(89)	2.024 003 ^b	1.966 597(88)	1.951 10(14)
$10^5 \times D_v$	3.483(20)	3.4 ^b	3.955(19)	7.649(89)
$10^8 \times H_v$	0.080(14)	0.075 ^b	0.287(13)	4.34(14)
$10^2 \times q_v$	0.810 7(48)	2.828(26)
$10^5 \times q_D$	-0.789(14)	-8.06(17)
$10^8 \times q_H$	0.340(94)	8.31(29)

^aUndetermined.

^bFixed values, see text for details.

TABLE V. Spectroscopic constants (in cm^{-1}) for the $d^3\Phi-a^3\Delta$ system of LaD.

Constants	$a^3\Delta_1$		$a^3\Delta_2$			$a^3\Delta_3$	
	$v=0$	$v=1$	$v=0$	$v=1$	$v=2$	$v=0$	$v=1$
B_v	1.933 785(30)	1.907 890(91)	1.949 845(53)	1.923 342(70)	1.896 81(19)	1.952 094(51)	1.925 28(15)
$10^5 \times D_v$	3.050 1(31)	3.108(32)	3.234(11)	3.274(16)	3.367(44)	3.166 9(65)	3.213(23)
$10^9 \times H_v$...	0.80(32)	0.466(73)	0.84(11)	2.563(57)	0.302(24)	0.62(11)
$10^3 \times q_v$	0.975 5(36)	1.163 3(76)
$10^7 \times q_{Dv}$	1.342(45)	1.58(15)
Constants	$d^3\Phi_2$		$d^3\Phi_3$			$d^3\Phi_4$	
	$v=0$	$v=1$	$v=0$	$v=1$	$v=2$	$v=0$	$v=1$
T_{v-v}	6006.5437(15)	5934.9798(19)	6267.0939(12)	6186.8252(16)	6106.3297(23)	6340.5031(20)	6260.3775(91)
B_v	1.833 100(30)	1.810 214(93)	1.841 828(56)	1.816 494(76)	1.791 99(19)	1.857 956(53)	1.830 31(15)
$10^5 \times D_v$	3.035 4(33)	3.044(32)	3.040(14)	3.199(20)	2.782(45)	3.333 6(66)	3.411(24)
$10^9 \times H_v$	0.192(12)	1.49(33)	-2.60(13)	6.09(21)	...	0.390(24)	0.80(12)
$10^{12} \times L_v$	3.337(48)	-2.15(10)

energy levels and the Ω -doubling constants are effective values that empirically account for some of the energy level splittings.

B. Spectrum of LaD

The spectra of LaH and LaD are almost identical in appearance. The LaD bands in the 4000–4350 cm^{-1} and 5600–6500 cm^{-1} regions are due to the $A^1\Pi-X^1\Sigma^+$ and $d^3\Phi-a^3\Delta$ transitions. A view of the compressed spectra of the $d^3\Phi-a^3\Delta$ transition is provided in Fig. 5 where the R and Q heads of the 0-0 bands of different subbands have been marked.

The bands with origins at 4547.5969(26) and 4472.7499(42) cm^{-1} have been identified as the 0-0 and 1-1 bands of the $A^1\Pi-X^1\Sigma^+$ transition. Again the 1-1 band is much weaker in intensity than the 0-0 band. There is a global perturbation in the $v=0$ vibrational level of the excited $A^1\Pi$ state which affects the lower J lines involving the e -parity levels. All the lines with $J' \leq 19$ were deweighted in the final fit although the corresponding combination differences for the unperturbed $X^1\Sigma^+$ state were included. In the 1-1 band only R and Q branches were identified so therefore the rotational constants for the $v=1$ vibrational level of the $X^1\Sigma^+$ state were fixed. The B_1 value was obtained from the B_0 value of LaD and the α_e value predicted using the isotopic relationship.³⁵ The table of the wave numbers of this transi-

tion is also available from PAPS³³ or from the authors. The molecular constants obtained are provided in Table IV.

The new bands observed to higher wavenumbers have been classified into three subbands with 0-0 band origins at 6006.5437(15), 6267.0939(12), and 6340.5031(20) cm^{-1} . These bands have been assigned as the $^3\Phi_2-^3\Delta_1$, $^3\Phi_3-^3\Delta_2$, and $^3\Phi_4-^3\Delta_3$ subbands of the $d^3\Phi-a^3\Delta$ transition. A part of the $^3\Phi_3-^3\Delta_2$ 0-0 band near the R head is provided in Fig. 6, in which some overlapping lines due to the $^3\Phi_4-^3\Delta_3$ 0-0 band have also been marked. A few low J lines of this subband also displayed hyperfine splitting of about the same magnitude as in LaH. The rotational analysis of the 0-0 and 1-1 bands of each subband has been obtained. The 2-2 band of the $^3\Phi_3-^3\Delta_2$ subband was also analyzed. The wave numbers of this transition are also available from PAPS³³ or from the authors. The rotational constants obtained for the $a^3\Delta$ and $d^3\Phi$ states are provided in Table V.

IV. DISCUSSION

The recent theoretical calculation of Das and Balasubramanian¹¹ predicts that the ground and most of the low-lying excited states of LaH arise from mixed configurations. For example the ground state is a mixture of 86% $1\sigma^2 2\sigma^2$, 6% $1\sigma^2 1\delta^2$, and 4% $1\sigma^2 1\pi^2$. According to this prediction there should be a $^1\Pi-^1\Sigma^+$ transition at about 6226 cm^{-1} , consistent with our observation of a $^1\Pi$ state at 4533 cm^{-1} . Similarly a $^3\Phi-^3\Delta$ transition is predicted at 7807 cm^{-1} which is again consistent with the observation of a $^3\Phi$ state at 6238 cm^{-1} above the $^3\Delta$ state. In addition there are several other allowed transitions predicted to lie between 10 000–20 000 cm^{-1} . Some of these have been observed by Bernard and Bacis and the rest are still to be investigated.

The hyperfine structure observed in the $a^3\Delta_3$ spin component gives some information about electronic configurations. The nominal configuration for the $X^1\Sigma^+$, $A^1\Pi$, $d^3\Phi$, and $a^3\Delta$ states are $1\sigma^2 2\sigma^2$, $1\sigma^2 2\sigma^1 d\pi^1$, $1\sigma^2 d\pi^1 d\delta^1$, and $1\sigma^2 2\sigma^1 d\delta^1$, respectively. Only the $A^1\Pi$ and $a^3\Delta$ states have

TABLE VI. Equilibrium constants (in cm^{-1}) for the $X^1\Sigma^+$ and $A^1\Pi$ states of LaH and LaD.

Constants	LaH		LaD	
	$X^1\Sigma^+$	$A^1\Pi$	$X^1\Sigma^+$	$A^1\Pi$
B_e	4.080 534(80)	3.915 776(81)	2.065 54(11)	1.974 35(12)
α_e	0.077 39(10)	0.078 25(10)	0.027 691 ^a	0.015 50(17)
r_e (Å)	2.031 969(20)	2.074 276(21)	2.027 527(54)	2.073 822(63)

^aFixed value, see text for details.

TABLE VII. Effective equilibrium constants (in cm^{-1}) for the $a^3\Delta$ and $d^3\Phi$ spin components of LaH and LaD.

Constants	LaH			LaD		
	$a^3\Delta_1$	$a^3\Delta_2$	$a^3\Delta_3$	$a^3\Delta_1$	$a^3\Delta_2$	$a^3\Delta_3$
B_e	3.820 71(16)	3.882 37(16)	3.889 608(73)	1.946 733(57)	1.963 10(12)	1.965 501(94)
α_e	0.072 64(17)	0.075 77(32)	0.079 935(89)	0.025 895(96)	0.026 52(22)	0.026 81(16)
r_e (Å)	2.099 924(44)	2.083 181(43)	2.081 242(19)	2.088 480(30)	2.079 756(64)	2.078 485(50)
Constants	LaH			LaD		
	$d^3\Phi_2$	$d^3\Phi_3$	$d^3\Phi_4$	$d^3\Phi_2$	$d^3\Phi_3$	$d^3\Phi_4$
B_e	3.650 40(16)	3.674 07(17)	3.733 104(76)	1.844 543(57)	1.854 29(13)	1.871 779(96)
α_e	0.072 21(17)	0.076 54(34)	0.080 493(94)	0.022 886(98)	0.024 92(23)	0.027 65(16)
r_e (Å)	2.148 351(47)	2.141 420(50)	2.124 420(21)	2.145 552(33)	2.139 906(75)	2.129 885(54)

unpaired $s\sigma$ character consistent with a relatively large hyperfine effect.³⁴ The hyperfine energy formula [Eq. (3)] also correctly predicts that, in general, the spin-component of a given term with the maximum Ω , Λ , and Σ values ($a^3\Delta_3$) should have the largest hyperfine splittings.

The rotational constants obtained from the $A^1\Pi-X^1\Sigma^+$ transition of LaH (Table II) and LaD (Table IV) have been used to evaluate the equilibrium rotational constants which are provided in Table VI. The equilibrium rotational constants have been used to evaluate the equilibrium bond lengths of the ground and excited states of LaH and LaD. The observed equilibrium bond lengths for the ground state of LaH and LaD are 2.031 969(20) and 2.027 527(54) Å, respectively. These values can be compared with the theoretical value of 2.08 Å predicted for LaH by Das and Balasubramanian.¹¹ The experimental r_e value for the $A^1\Pi$ state of LaH is 2.074 276(21) Å, to be compared with the prediction¹¹ of 2.13 Å.

The rotational constants for the $a^3\Delta$ and $d^3\Phi$ states of LaH and LaD have also been used to determine the equilibrium constants for the individual spin-components of these states. The effective equilibrium constants for the $^3\Delta$ and $^3\Phi$ states of LaH and LaD are provided in Table VII. The *ab initio* values¹¹ of r_e are 2.13 Å for the $^3\Delta$ state and 2.16 Å for the $^3\Phi$ state. Note that the experimental $a^3\Delta$ constants show evidence of mixing with other states such as the nearby $^1\Delta$ and $^3\Pi$ states.

V. CONCLUSION

The infrared spectra of LaH and LaD have been investigated in the 1 μm –3 μm spectral region using a Fourier transform spectrometer. The bands observed have been classified into two new electronic transitions; $A^1\Pi^+-X^1\Sigma^+$ and $d^3\Phi-a^3\Delta$. The analyses of these bands provide a set of principal molecular constants for the ground $X^1\Sigma^+$ and the excited $A^1\Pi$, $a^3\Delta$, and $d^3\Phi$ states of LaH and LaD. We assign our new $^1\Sigma^+$ state as the ground state of LaH as predicted by Das and Balasubramanian,¹¹ although we have no direct experimental proof.

ACKNOWLEDGMENTS

We thank J. Wagner and C. Plymate of the National Solar Observatory for assistance in obtaining the spectra. The National Solar Observatory is operated by the Association of Universities for Research in Astronomy, Inc., under contract with the National Science Foundation. The research described here was supported by funding from the Petroleum Research Fund administered by the American Chemical Society. Support was also provided by the Natural Science and Engineering Research Council of Canada and the NASA laboratory astrophysics program.

- ¹C. J. Cheetham and R. F. Barrow, *Adv. High Temp. Chem.* **1**, 7 (1967).
- ²R. E. Smith, *Proc. R. Soc. London, Ser. A* **332**, 113 (1973).
- ³P. R. Scott and W. G. Richards, *Chem. Soc. Specialist Periodical Reports* **4**, 70 (1976).
- ⁴P. B. Armentrout and L. S. Sunderlin, *Acc. Chem. Res.* **22**, 315 (1989).
- ⁵C. W. Bauschlicher and S. R. Langhoff, *Acc. Chem. Res.* **22**, 103 (1989).
- ⁶R. Yerle, *Astron. Astrophys.* **73**, 346 (1979).
- ⁷B. Lindgren and G. Olofsson, *Astron. Astrophys.* **84**, 300 (1980).
- ⁸P. K. Carroll, P. McCormack, and S. O'Connor, *Astrophys. J.* **208**, 903 (1976).
- ⁹D. L. Lambert and E. A. Mallia, *Mon. Not. R. Astron. Soc. London* **151**, 437 (1971).
- ¹⁰O. Engvold, H. Wöhl, and J. W. Brault, *Astron. Astrophys. Suppl. Ser.* **42**, 209 (1980).
- ¹¹K. K. Das and K. Balasubramanian, *Chem. Phys. Lett.* **172**, 372 (1990).
- ¹²K. Balasubramanian and K. K. Das, *J. Mol. Spectrosc.* **145**, 142 (1991).
- ¹³W. Cheng and K. Balasubramanian, *J. Mol. Spectrosc.* **149**, 99 (1991).
- ¹⁴Z. Ma and K. Balasubramanian, *Chem. Phys. Lett.* **181**, 467 (1991).
- ¹⁵D. Dai and K. Balasubramanian, *J. Mol. Spectrosc.* **158**, 455 (1993).
- ¹⁶M. Benavides and K. Balasubramanian, *J. Mol. Spectrosc.* **150**, 271 (1990).
- ¹⁷D. Dai and K. Balasubramanian, *New J. Chem.* **15**, 721 (1991).
- ¹⁸T. Fleng and C. M. Marian, *Chem. Phys. Lett.* **222**, 267 (1994).
- ¹⁹A. Piezlo, G. Jansen, B. A. Hess, and W. Niessen, *J. Chem. Phys.* **98**, 3945 (1993).
- ²⁰R. Bacis, A. Bernard, and A. Zgainski, *C. R. Acad. Sci. B* **280**, 77 (1975).
- ²¹A. Bernard and R. Bacis, *Can. J. Phys.* **54**, 1509 (1976).
- ²²R. S. Ram and P. F. Bernath, *J. Chem. Phys.* **101**, 74 (1994).
- ²³J. F. Garvey and A. Kuppermann, *J. Phys. Chem.* **92**, 4583 (1988).
- ²⁴M. C. McCarthy, R. W. Field, R. Engleman, and P. F. Bernath, *J. Mol. Spectrosc.* **158**, 208 (1993).
- ²⁵U. Ringstrom, *Ark. f. Fys.* **27**, 227 (1964).
- ²⁶R. S. Ram and P. F. Bernath, *J. Chem. Phys.* **101**, 9283 (1994).
- ²⁷L. Kaledin, J. E. McCord, and M. C. Heaven, *J. Opt. Soc. Am. B* **11**, 219 (1994).
- ²⁸J. Anglada, P. J. Bruna, and S. D. Peyerimhoff, *Mol. Phys.* **66**, 541 (1989).

- ²⁹S. R. Langhoff, L. G. M. Pettersson, C. W. Bauschlicher, and H. Partridge, *J. Chem. Phys.* **86**, 268 (1987).
- ³⁰K. Balasubramanian and J. Z. Wang, *J. Mol. Spectrosc.* **133**, 82 (1989).
- ³¹B. A. Palmer and R. Engleman, *Atlas of the Thorium Spectrum* (Los Alamos National Laboratory, Los Alamos, 1983).
- ³²H. Schall, M. Dulick, and R. W. Field, *J. Chem. Phys.* **87**, 2898 (1987).
- ³³See AIP document no. PAPS JCPSA-104-6444-12 for 12 pages of data tables. Order by PAPS number and journal reference from American Institute of Physics, Physics Auxiliary Publication Service, Carolyn Gehlbach, 500 Sunnyside Boulevard, Woodbury, New York 11797-2999. Fax: 516-576-2223, e-mail: janis@aip.org. The price is \$1.50 for each microfiche (98 pages) or \$5.00 for photocopies of up to 30 pages, and \$0.15 for each additional page over 30 pages. Airmail additional. Make checks payable to the American Institute of Physics.
- ³⁴T. M. Dunn, in *Molecular Spectroscopy-Modern Research*, edited by K. N. Rao and C. W. Mathews (Academic, New York, 1972), p. 231.
- ³⁵G. Herzberg, *Spectra of Diatomic Molecules* (Van Nostrand, New York, 1950).
- ³⁶R. F. Barrow, M. W. Bastin, D. L. G. Moore, and C. J. Pott, *Nature* **215**, 1072 (1967).